The 2010 IEEE/RSJ International Conference on
Intelligent Robots and Systems
October 18-22, 2010, Taipei, Taiwan

Electromyographic Signal Integrated Robot Hand Control for Massage Therapy Applications

Ren C. Luo and Chih C. Chang

Abstract—**This paper presents an electromyographic (EMG) signal integrated multi-finger robot hand control for massage applications. This research explores the feasible application of multi-finger robot hands except for the use as prostheses and grasping applications. The forearm EMG of a person who is massaged by the human hands is recorded and analyzed statistically. First, the root mean square (RMS) of the raw data is computed as the discrimination between normal and contracted states of the muscle. Then the EMG signal at contracted state is further divided into painful and comfortable groups based on the impulse factor which is defined to estimate the sharpness of waveform variations. As a consequence, two discriminative values of the EMG signal are generated to distinguish painful and comfortable feelings. Based on the relationship between the human feeling and the massage force, we get an appropriate range of input commands of the robot hand for massage applications. A grasp-kneading massage is performed on the human shoulder to verify the proposed process. As a result, an effective and comfortable massage using the multi-finger robot hand is realized.**

I. Introduction

ELECTROMYOGRAM is a measurement of the electrical activity of muscles at resting state and during contraction. It is originally used to monitor and diagnose the electrical features of special muscles for medical care. Currently, it is applied in engineering fields more and more often. For instance in robotic applications, EMG potentials generated by forearm muscles can be extracted to control an artificial prosthetic robot hand [1,2]. Although the use of EMG signals in a robotic system has advantages of non-invasive measurements and providing physiological information, the main problems in the development are vague features and large variations in signals. As summarized in [3], a common process dealing with EMG signals includes data segmentation, feature extraction, and classification.

Multi-finger robot hands have been used for many applications such as dexterous manipulation and prostheses. For instance, the Gifu hand [4] and the DLR hand I and II [5,6] with anthropomorphic configuration and multiple sensors are developed for dexterous manipulations. The CyberHand [7] and i-Limb hand [8] are developed for the use as prostheses. In addition to these applications, multi-finger robot hands can also be used for massage purposes. Massage is a popular treatment of body conditioning and physical therapy in eastern Asian countries such as China and Japan. It has been validated that many health benefits can be achieved through massage, such as improved blood circulation, lowered blood pressure, reduced heart rate, relief from fatigue, relaxed muscle tone, etc. Some research efforts on the massage issue are presented in literature [9-13]. In the development of a massage robot system, the robot is expected to provide a safe as well as comfortable massage therapy. So the human user's feeling must be taken into account to help controlling the massage according to differing physical conditions. Kazuya Hiyamizu et al. [17] developed a human sensory sensor and integrated it to the massage chair. The developed sensor measures the peripheral skin temperature, pulse, and galvanic skin response simultaneously to estimate human sensations such as comfortable/uncomfortable or relaxed/tense. The estimated result is used to control the massage action instantaneously. In addition to these used physiological quantities, EMG is considered a valuable information in massage applications since it provides more direct information about the muscle conditions. Daniele F. Zullino et al. [14] reported an evaluation of the EMG variation caused by massage using a massage chair. For this reason, we attempt to integrate extracted EMG features to the control of the robot hand for massage applications. The goal of this research is to determine adequate values of the input command of the robot hand via analyzing EMG signals of a person who is massaged by the human hands. By this way, the massage robot can provide people with comfortable therapy using a proper massaging force. Differing in use from prostheses to grasping tools, the multi-finger hand of the massage robot opens up a new application field.

This paper is organized as follows. Section II provides an overview of the EMG signal integrated massage robot system, section III presents the dynamics of the robot hand interacting with the human body, section IV shows the analysis and characterization of EMG signals, experimental results and discussion are shown in section V, and section VI gives a conclusion and propose some future works on the massage robot system.

II. Overview of the Massage Robot System

A. Overview of the Massage Robot System

Fig. 1(a) is a conceptual computer model of the massage robot system. The robot is designed to anthropomorphic shape. It is equipped with a pair of robot arms, each fitted with 7 degree of freedoms (DOF) for dexterous motion. A

Ren C. Luo is with the National Taiwan University, Taipei 10617, Taiwan, (email: renluo@ntu.edu.tw)
Chih C. Chang is with the National Taiwan University, Taipei 10617, Taiwan, (email: cchang@ira.ee.ntu.edu.tw)

critical consideration in human-robot coexistence application is the safety of operation, to this end, the designed arm has variable stiffness joints at shoulder and elbow. The safety arm can automatically release the momentum by changing the mechanical stiffness of the actuator, such that the robot can avoid hurting the human subject should an undesired collision occur.

(a) (b)

Fig. 1 (a)Conceptual computer model of the massage robot system. (b)Mechanism of the robot hand.

As shown in Fig. 1(b), the robot hand has 3 fingers and 1 thumb, each one with 2 joints and in total 8 DOFs. The total length of the robot hand from the wrist to the fingertip is about *300mm*, and the extended width is about *285mm*. For an anthropomorphic robot hand the size seems to be a little bit large, it is an unavoidable trade-off due to the requirement of high output forces.

The four-finger robot hand is attached to the wrist as the effectors of the massage. The designed robot hand is actuated by built-in DC servomotors which are arranged in the palm and fingers. The specifications of the selected motor with reduction gear and encoder are listed in Table I. Despite the lower maximum output force when compared with tendon-driven robot hands, the motor built-in mechanism possesses advantages of more compact structure and more robust control performances.

TABLE I
SPECIFICATION OF DC MOTOR (maxon A-max 22)

Motor Data	Value	
Nominal voltage	12.0	V
Nominal speed	6990	rpm
Nominal torque	6.77	mNm
Stall torque	22.8	mNm
Nominal current	0.664	A
Diameter	22	mm
Total length (+ gearhead + encoder)	80.0	mm

The principal designing consideration of the massage robot hand is the high output force. An adult male who wears a sensory glove (TouchGlove, I-CubeX) performs the grasp-kneading massage on the subject's shoulder and the forces are recorded. The common massage force measured is about 20N at least, this is much higher than what the majority of existing multi-finger robot hands can currently offer. To generate higher output force in this research, a gearhead with a reduction ratio of 389:1 is selected. With the configuration, a maximum force of 42N can be generated at the fingertip for short term operation, and the operating speed is 108 degrees per second. For the consideration of rigid and compact mechanism, the designed fingers are constructed with only two phalanges where the distal phalange is removed. Since this robot hand is used to perform massage motions similar to power grasps, the adduction/abduction function of the human finger is not imperative so the finger possesses only the flexure/extension function. Typical massage motions include kneading, pressing, tapping, rolling and rubbing. The developed anthropomorphic robot hand can perform most massage motions dexterously when it is integrated with the safety robot arm in our future works.

An important component in the massage robot system is the electromyograph (BioRadio 150, Cleveland Medical Devices Inc.). The integration of EMG information in the system is used for the following purposes.

1) Massage force setting

Base on the characterization of the EMG signals measured during the human hand massage, the massage force of the robot hand is constrained in an adequate range for comfortable massages.

2) Massage effect evaluation

By comparing parameters of EMG signals such as electrical amplitude (EA) and median frequency (MF) before and after the massage, the therapeutical effect of the massage can be quantitatively evaluated.

3) Real-time massage monitoring

The original concept of the developed EMG-integrated massage robot system is to control the massage actions under the online EMG monitoring. By measuring and analyzing the EMG signals continuously during massage, the massaging force output of the robot hand can be modulated according to the human sensation. The main challenges include the identification of pain by detecting EMG from other muscles which is away from the massaged region, and the integration problem of different device interfaces.

B. Experimental Process

Development of the massage robot system attempts to improve the performances of commercial massage chairs. According to our experiments, it is observed that the EMG potential varies with the contracting level of the muscle and shows a sharp variation when pain occurs. The key idea of this research is to identify the relationship between EMG signal features and corresponding massage forces when a person is massaged by a massage specialist. Then the thresholds of input command to the actuator are determined according to the extracted features - so that the output force is constrained by the thresholds and the robot hand can operate in a proper manner. Fig. 2 illustrates the experimental process.

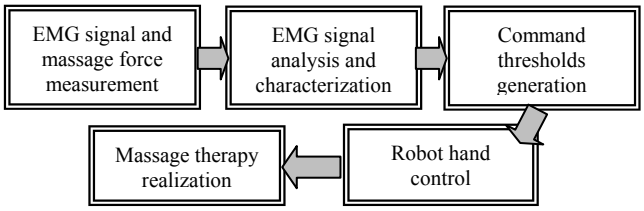

Fig. 2 Experimental process.

III. DYNAMICS OF THE ROBOT HAND INTERACTING WITH THE HUMAN BODY

Fig. 3 shows the configuration of a finger module. The world coordinate frame *W* is attached to the wrist while the manipulator coordinate frame *E* is attached to the fingertip. The joint angle vector $q = (q_1, q_2)^T$ represents the amounts of rotation at revolute joints respectively, and $\omega_n \in R^3, n = 1,2$ are unit vectors at rotational axes. l_i , *i*=1 to 3, represent lengths of phalanges from the wrist to the fingertip.

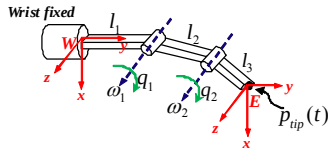

Fig. 3 Configuration of the finger with an amount of rotation.

Here the typical dynamic equation of a robot manipulator based on Lagrange's equations is used. Considering inertial, centrifugal and Coriolis forces and gravity of the mechanical system with external forces exerting on actuators, Lagrange's equations result in equation (1).

$$I(q)\ddot{q} + C(q,\dot{q})\dot{q} + G(q) = \tau \tag{1}$$

Where $I(q)$ is the inertial matrix, $C(q,\dot{q})$ is the Coriolis and centrifugal matrix, $G(q)$ represents the gravity effect, and τ is generated torques at the joints. When the robot hand interacts with the human body, torques exerting on the actuator include the torque generated itself and the torque caused by the reactive force. It follows equation (2) with the actuator torque τ_{act} and the reactive torque τ_{rea} .

$$\tau = \tau_{act} + \tau_{rea} \tag{2}$$

Define the transfer function $f_{WE}(q)$ which maps $p_{tip}(t)$ and q in the product of exponentials form as equation (3).

$$f_{WE}(q) = e^{\hat{\xi}_1 q_1} e^{\hat{\xi}_2 q_2} f_{WE}(0) \tag{3}$$

The subscript of $f_{WE}(q)$ indicates the transformation from frame *E* to *W*. In this equation, $\hat{\xi}_n$ in homogeneous form are twists at rotational axes, and $f_{WE}(0)$ is the transformation of the initial configuration with fingers stretched.

The reactive torque τ_{rea} in equation (2) is generated by the interactive force at the fingertip through the Jacobian transformation. That is $\tau_{rea} = J_{WE}(q)F_{rea}$, where F_{rea} is the reactive force which occurs at the interacting region between the fingertip and the human body. And the Jacobian $J_{WE}(q)$ is formulated by differentiating the forward kinematics map, that is $J_{WE}(q) = \dfrac{\partial f_{WE}(q)}{\partial q}$ herein.

With the substitution, the manipulator dynamic equation (1) can be rewritten as equation (4).

$$I(q)\ddot{q} + C(q,\dot{q})\dot{q} + G(q) = \tau_{act} + J_{WE}(q)F_{rea} \tag{4}$$

During massage, the robot hand presses the human muscle physically. The muscle can be modeled as a simple mass-damper-spring system with M_m , D_m and K_m representing matrices of the mass, damping and stiffness respectively. Given the position error of the fingertip $\tilde{p}_{tip} = \hat{p}_{tip} - p_{tip}$ where $\hat{p}_{tip}$ is the desired trajectory, the dynamic equation of the human muscle is formulated as equation (5).

$$M_m\ddot{\tilde{p}}_{tip} + D_m\dot{\tilde{p}}_{tip} + K_m\tilde{p}_{tip} = F_{rea} \tag{5}$$

By combining equation (4) and (5), the required control input of joint torque for interaction is derived as equation (6).

$$\begin{aligned}\tau_{act} = I(q)J_{WE}(q)^{-1}\{M_m^{-1}[F_{rea} - D_m\ddot{\tilde{p}}_{tip} \\ - K_m\tilde{p}_{tip}] - \dot{J}_{WE}(q)\dot{q}\} + C(q,\dot{q})\dot{q} \\ + G(q) - J_{WE}(q)^T F_{rea}\end{aligned} \tag{6}$$

IV. EMG SIGNALS ANALYSIS AND CHARACTERIZATION

As our previous work mentioned [16], the object of using analyzed EMG information in the robot hand control scheme is to enhance the safety and comfort of the massage therapy. Since EMG signals are extremely sensitive to neural stimuli, it is feasible to detect a sign of pain from the person who is suffering an uncomfortable massage. Instead of experiential setting of massage parameters in massage chairs, this research aims to schedule control commands of the robot hand according to the analyzed electromyographic information.

A. Characterization of Human Feelings

Fig. 4 shows the EMG signal of the forearm muscle. It is measured under this situation: the massager exerts a periodical but varying force magnitude grasp-kneading on the shoulder of the user. At time t_1, t_2, t_3 and t_4, the muscle generates higher electrical pulses due to the grasp-kneading. Moreover, at time t_2 a more sharp variation of EMG amplitude is observed while the massager enhances the massaging force deliberately and the user feels an unbearable pain.

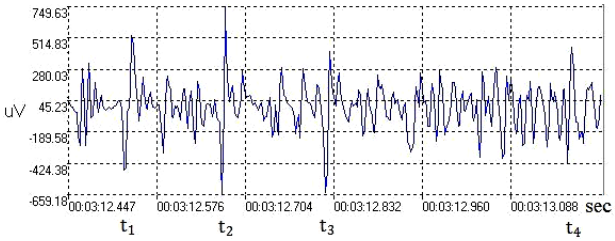

Fig. 4 EMG signal of the forearm. Max. potential: 749.63μV. Min. potential: -659.18μV. Duration: 0.77seconds.

It is found that grasp-kneading massage on the shoulder causes variations in the EMG signal measured from the forearm muscle, and the time instant of painful feeling is consistent with an excessive grasp-kneading force. We intend to get an adequate range of massaging forces by analyzing the measured EMG signals. Fig. 5 is a conceptual graph of the relationship between the EMG potential and the feeling characterization. Where V_{EMG} is the electrical potential of EMG while V_{th}^{H} and V_{th}^{L} represent higher and lower thresholds of a comfortable massage respectively.

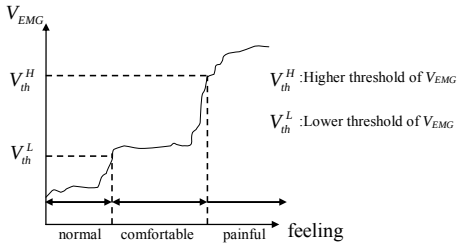

Fig. 5 Conceptual graph of the EMG characterization.

B. EMG Analysis

This section shows how we analyze the EMG data in Fig. 5 to generate the desired thresholds in Fig. 6.

1) Rectification of EMG

The EMG signal is rectified first. Let V_i denotes the *i*-th EMG potential at time step *i*, the rectification is simply takes the absolute value of V_i , named $\overline{V_i}$.

2) Discrimination of stimulated EMG

To have an effective massage, the lower threshold V_{th}^{L} must be greater than the normal voltage of the muscle. Herein, the root mean square of all the data is adopted. Moreover, properties of EMG are different according to the muscle type, a scaling factor β which is tuned experimentally is multiplied by the RMS. It follows equation (7), where *n* is the amount of raw data.

$$V_{th}^{L} = \beta \cdot \left(\frac{1}{n} \sum_{i=1}^{n} \overline{V_i}^2 \right)^{\frac{1}{2}} \tag{7}$$

3) Filtering

After the lower threshold V_{th}^{L} is obtained, the data points with $\overline{V_i} < V_{th}^{L}$ are filtered. Then the remainders form several spikes above the threshold.

4) Characterization of the muscle contraction

The experimental results show that the EMG signal reflects the pain with a sharp variation. In other words, when the pain occurs, an electromyographic output with high amplitude but small time period pops up in the EMG waveform. To characterize this, assume j (j<n) spikes exist, let $V_j^{\max}$ denotes the maximum voltage during the *j*-th spike, and Δt_j represents the data number in the *j*-th spike namely the *j*-th transversal region. An impulse factor r_j is defined in equation (8).

$$r_j = \frac{V_j^{\max} - V_{th}^{L}}{\Delta t_j} \tag{8}$$

According to these computed impulses, similar to step 2 the stimulated EMG can be divided into two groups, namely the painful group and the comfortable group. Let r_{pai}^{rms} and r_{com}^{rms} represent the impulse factor RMS of the painful and comfortable groups respectively. The higher threshold V_{th}^{H} is obtained by comparing RMS and boundaries of these two groups as depicted in Fig. 6.

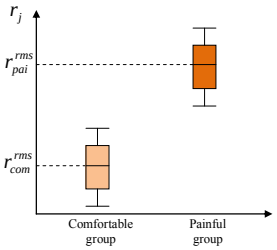

Fig. 6 Impulse factors of the comfortable and painful group.

Here the average of RMS calculated by equation (9) is used as the discriminating impulse factor called r_{th}^{H} .

$$r_{th}^{H} = \frac{r_{pai}^{rms} + r_{com}^{rms}}{2} \tag{9}$$

Finally, the higher threshold V_{th}^{H} can be derived by substituting r_{th}^{H} for r_j in equation (8).

V. Experimental Results

The experiment is carried out by the process presented in Fig. 3. It starts with EMG measurement and analysis, where the forearm EMG is measured when the shoulder is massaged by the human hand. Then the control parameters of the robot hand are decided according to the EMG thresholds. And the grasp-kneading massage is realized on a person's shoulder.

A. EMG Analysis and Characterization

The EMG signals of the subject are measured using a wireless electromyograph. Two silver/silver chloride electrodes are attached about one inch apart above the muscle, and one electrode is attached to the bony part as the ground electrode. The sampling rate is 960 Hz. Fig. 7 shows the setup of experiments. The portable user unit is responsible for amplifying, sampling and digitizing the acquired EMG signals and then wirelessly transmits them to the computer unit. The computer unit receives the data and connects to a USB port of the PC. To find the response of pain in EMG, six different muscles including frontalis, human back, bicep, forearm, vastus lateralis and gastrocnemius have been measured. The EMGs of frontalis and forearm muscles are more sensitive to the grasp-kneading effect. So the EMG signals of frontalis and forearm muscles are adopted here.

The frontalis has less muscle fibers but the detected EMG variation caused by pain is most obvious. This is because when a person feels painful suddenly, he always frowns automatically so that the EMG signal is disturbed due to the electrodes moving. Although the sharp variation in frontalis EMG does not reflect the real state of the muscle, it is actually a good index of pain. The frontalis EMG is measured for reference in every experiment.

Fig. 7 EMG measurement setup.

The experimental results of the proposed EMG analysis and characterization processes are shown in Fig. 8. The analyzed EMG signal is the same with that in Fig. 4. The number of processed data, the variable *n* in equation (7), is 500. Fig. 8(a) is the raw data and (b) is the rectified data. The green line in Fig. 8(c) represents the calculated value of the lower threshold V_{th}^{L} in equation (7) with β=0.8. And Fig. 8(d) shows the calculated impulse factors. By translating thresholds of impulse factors, the threshold values V_{th}^{L} (green line) and V_{th}^{H} (red line) of the originally electrical data are generated in Fig. 8(e). The experimental results of characterization are listed in Table II.

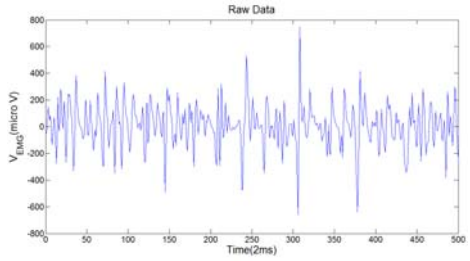

(a)

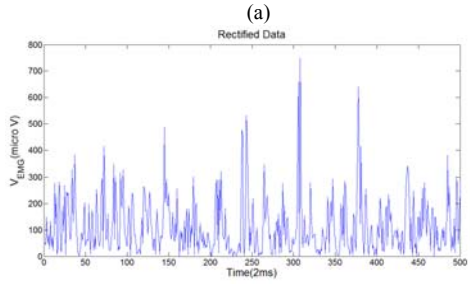

(b)

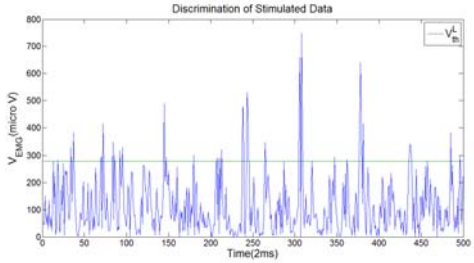

(c)

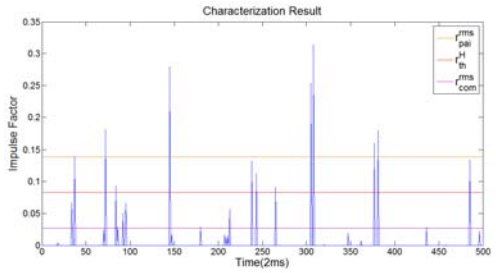

(d)

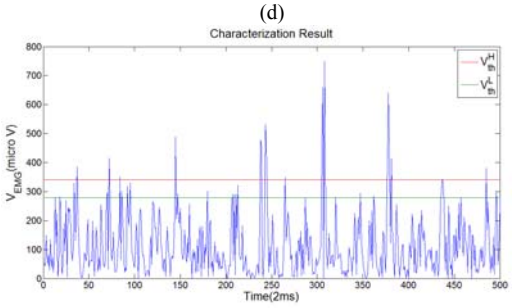

(e)

Fig. 8 Experimental results of EMG analysis and characterization. (a) Raw data. (b) Rectified data. (c) Discrimination of stimulated data. (d) Characterization result of impulse factor. (e) Characterization result of original rectified EMG.

TABLE II
CHARACTERIZATION RESULTS

Notation	Description	Value
r_{pai}^{rms}	Impulse factor RMS of painful group	0.1388
r_{com}^{rms}	Impulse factor RMS of comfortable group	0.0268
r_{th}^{H}	Impulse factor for higher threshold	0.0828
V_{th}^{H}	Higher threshold of EMG	341.4582μV
V_{th}^{L}	Lower threshold of EMG	279.3972μV

B. Grasp-kneading Massage by Robot Hand

The robot hand is controlled by a CAN bus control system through an USB CAN master (high-speed USB CAN interface, NI) connected to the PC. Based on the analyzed EMG information, the grasp-kneading massage using the robot hand is scheduled. Initially, the robot hand approaches the human body gently. When the robot hand contacts with the human body, the controller continuously reads the encoder data and checks if thresholds of actuating current and limited position are reached. The limitations of current and position are set according to the EMG analysis. Once one of them is detected, the current and position are set as parameters of the grasp-kneading motion control. After that, the robot hand exerts grasp-kneading upon the shoulder of a male who is 180cm in height and 85kg in weight.

Fig. 9 shows the experiment of grasp-kneading massage. In Fig. 9(a) the robot hand is in the initial configuration and is ready for approaching, (b) and (c) are kneading cycles, and (d)

shows the front view while massaging. During massage, the massaging forces can be calculated directly using the measured currents of encoders. The actuating currents and corresponding forces at four fingertips are listed in Table III. One can see that forces at the thumb, index finger and middle finger are similar and the force at the third finger is relatively lower. This is because index and middle fingers are more close to the opposition to thumb. Moreover, the third finger locates on the position of thinner muscles. As introduced in section II, the common massaging force is about 20N. Herein, the forces exerted on the shoulder are slightly lower, this is adjusted because of the consideration for the users' safety. But from the user's subjective sensation, the user still has an effective and comfortable massage without any pain.

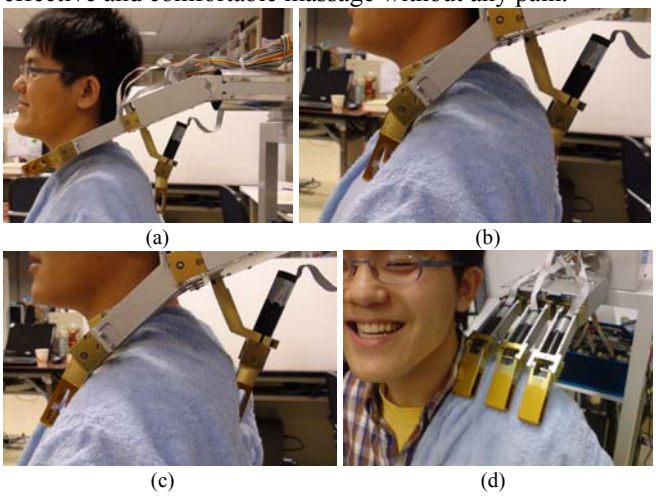

(a) (b) (c) (d)

Fig. 9. Experimental results of grasp-kneading massage. (a)ready for approaching; (b)pressing; (c)releasing; (d)front view.

TABLE III
MEASURED FORCES OF GRASP-KNEADING MASSAGE

Item	Encoder Current (mA)	Fingertip Force (N)
Thumb	617	12.32
Index finger	635	12.68
Middle finger	672	13.42
Third finger	520	10.38

VI. CONCLUSIONS

In this paper we present a massage robot system which is integrated with analyzed EMG information. By characterizing the human feeling of pain or comfort, the robot hand performs a grasp-kneading massage with proper force upon the human shoulder. The proposed process is verified by experimental results.

In the future, we will continue making efforts on the EMG analysis and pain identification with relevant algorithms to promote the reliability and repeatability of the proposed massage robot system. Further experiments including online monitoring and massage effect evaluation using EMG information will be carried out.

REFERENCES

[1] Y. Su, M. H. Fisher, A. Wolczowski, G. D. Bell, and R. X. Gao, "Towards an EMG-controlled prosthetic hand using a 3-D electromagnetic positioning system," *IEEE Trans. on Instrumentation and Measurement*, vol. 56, no. 1, Feb. 2007, pp. 178-186.

[2] S. Bitzer and P. van der Smagt, "Learning EMG control of a robotic hand: towards active prostheses," *Proc. of IEEE Int. Conf. on Robotics and Automation*, May 2006, pp. 2819-2823.

[3] M. A. Oskoei and H. Hu, "Myoelectric control systems- a survey," *Biomedical Signal Processing and Control*, vol. 2, no. 4, Oct. 2007, pp. 275-294.

[4] H. Kawasaki, T. Komatsu and K. Uchiyama, "Dexterous anthropomorphic robot hand with distributed tactile sensor: Gifu hand II," *IEEE/ASME Trans. on Mechatronics*, vol. 7, no. 3, Sep. 2002, pp. 296-303.

[5] H. Liu, P. Meusel, N. Seitz, B. Willberg, G. Hirzinger, M. H. Jin, Y. W. Liu, R. Wei and Z. W. Xie, "The modular multisensory DLR-HIT-Hand," *Mechanism and Machine Theory*, vol. 42, no. 5, May 2007, pp. 612-625.

[6] H. Liu, K. Wu, P. Meusel, N. Seitz, G. Hirzinger, M. H. Jin, Y. W. Liu, S. W. Fan, T. Lan and Z. P. Chen, "Multisensory five-finger dexterous hand: The DLR/HIT Hand II," *IEEE/RSJ Int. Conf. on Intelligent Robots and Systems*, Sept. 2008, pp. 3692-3697.

[7] M. C. Carrozza, G. Cappiello, S. Micera, B. B. Edin, L. Beccai and C. Cipreiani, "Design of a cybernetic hand for perception and action," *Biological Cybernetics*, vol. 95, no. 6, Dec. 2006, pp. 629-644.

[8] http://www.touchbionics.com/index.php

[9] M. Kume, Y. Morita, Y. Yamauchi, H. Aoki, M. Yamada and K. Tsukamoto, "Development of a mechanotherapy unit for examining the possibility of an intelligent massage robot," *Proc. of the IEEE/RSJ Int. Conf. on Intelligent Robots and Systems*, vol. 1, Nov. 1996, pp. 346-353.

[10] K. C. Jones and W. Du, "Development of a massage robot for medical therapy," *Proc. of IEEE/ASME Int. Conf. on Advanced Intelligent Mechatronics*, vol. 2, July 2003, pp. 1096-1101.

[11] H. Koga, Y. Usuda, M. Matsuno, Y. Ogura, H. Ishii, J. Solis, A. Takanishi and A. Katsumata, "Development of oral rehabilitation robot for massage therapy," *6th Int. Special Topic Conf. on Information Technology Applications in Biomedicine*, Nov. 2007, pp. 111-114.

[12] P. Minyong, T. Miyoshi, K. Terashima and H. Kitagawa, "Expert massage motion control by multi-fingered robot hand," *IEEE/RSJ Int. Conf. on Intelligent Robots and Systems*, Oct. 2003, pp. 3035-3040.

[13] K. Terashima, H. Kitagawa, T. Miyoshi, P. Minyong and T. Kondo, "Modeling and massage control of human skin muscle by using multi-fingered robot hand," *Integrated Computer-Aided Engineering*, vol. 13, no. 3, 2006, pp. 233-248.

[14] D. F. Zullino, S. Krenz, E. Frésard, E. Cancela and Y. Khazaal, "Local back massage with an automated massage chair: General muscle and psychophysiologic relaxing properties," *Journal of Alternative and Complementary Medicine*, vol. 11, no. 6, 2005, pp. 1103-1106.

[15] R. M. Murray, Z. Li and S. S. Sastry, "A mathematical introduction to robotic manipulation," Florida: CRC, 1994.

[16] R. C. Luo, C. C. Chang, and Y. W. Perng, "Impedance control on a multi-fingered robot hand based on analyzed electromyographic information for massage applications," *IEEE Int. Symposium on Industrial Electronics*, 2009, pp. 1228-1233.

[17] K. Hiyamizu, Y. Fujiwara, H. Genno, M. Yasuda and T. Koma, "Development of human sensory sensor and application to massaging chairs," *Proc. of IEEE Symp. on Computational Intelligence in Robotics and Automation*, July 2003, pp. 140-144.